

*Electronic Supplementary Information for*

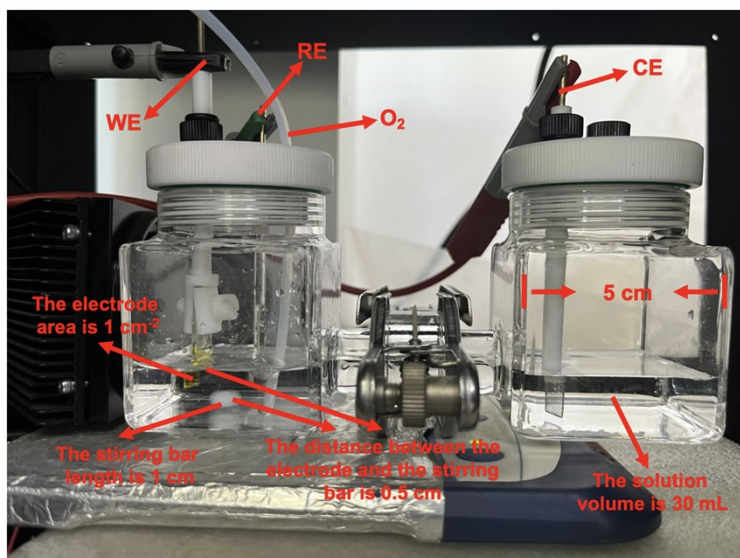
**Multipoint-bridging structure with piezoelectric-induced S-scheme  
junction for piezoelectrically-enhanced photoelectrochemical H<sub>2</sub>O<sub>2</sub>  
production**

Chenpu Chen, Jun Cheng\*

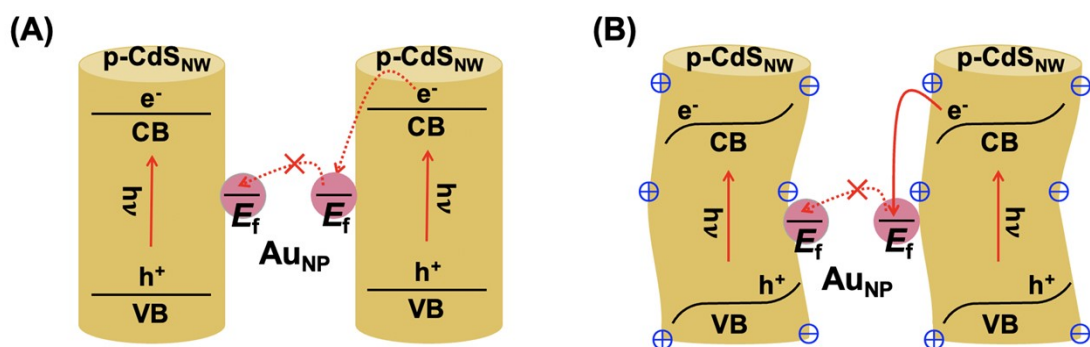
Key Laboratory of Chemical Biology & Traditional Chinese Medicine Research (Ministry of Education of China), College of Chemistry and Chemical Engineering, Hunan Normal University, Changsha 410081, China

---

\*Corresponding author.  
E-mail address: [cj1006@hunnu.edu.cn](mailto:cj1006@hunnu.edu.cn) (J. Cheng).



**Scheme S1.** Device image of the PPEC-ORR. Here, the side length of the PEC cell is 5 cm, the solution volume is 30 mL, the electrode area is 1 cm<sup>2</sup>, the stirring bar length is 1 cm, and the distance between the electrode and the stirring bar is 0.5 cm.



**Scheme S2.** Illustration of the energy band structures and the possible electron-transfer pathways on the  $\text{Au}_{\text{NP}}/\text{p-CdS}_{\text{NW}}/\text{ITO}$  electrode in an unstirred (A) or 1500-rpm-stirred (B)  $\text{O}_2$ -saturated 0.5 M aqueous  $\text{Na}_2\text{SO}_4$  under  $100 \text{ mW cm}^{-2}$  AM 1.5G simulated sunlight illumination. Here, although solution stirring can bend the  $\text{p-CdS}_{\text{NW}}$  to generate piezoelectric charges and interleave the energy band positions of two adjacent  $\text{p-CdS}_{\text{NW}}^1$ , the spatial distance between the  $\text{p-CdS}_{\text{NW}}$  is sufficiently large and there is no transverse electron conductor bridge. Therefore, transverse electron transfer between adjacent  $\text{p-CdS}_{\text{NW}}$  is not possible (dashed arrows).

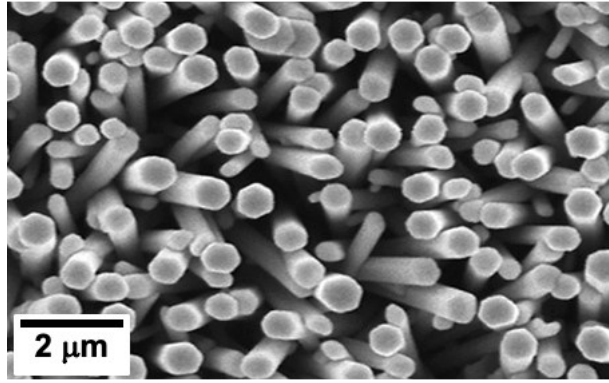


**Fig. S1.** SEM image of n-CdS<sub>NW</sub>/ITO electrode.

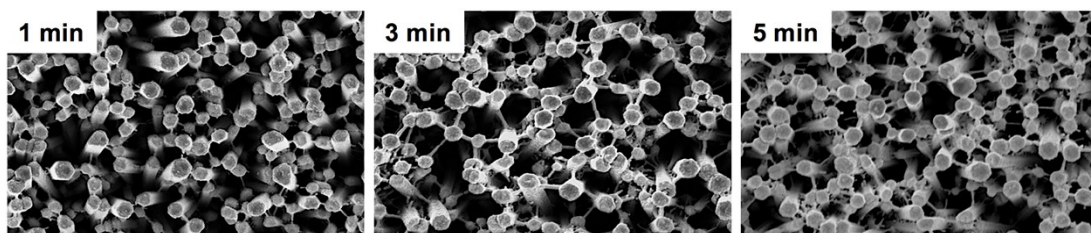


**Fig. S2.** SEM images of the  $\text{Au}_{\text{NR}}/\text{p-CdS}_{\text{NW}}/\text{ITO}$  electrodes prepared by photodeposition of  $\text{Au}_{\text{NR}}$  at different times.

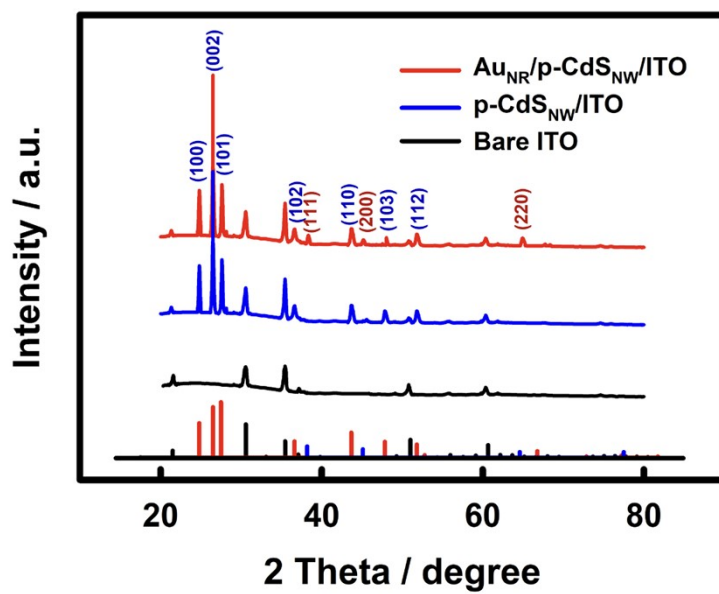


**Fig. S3.** XRD patterns of the bare ITO, p-CdS<sub>NW</sub>/ITO and Au<sub>NR</sub>/p-CdS<sub>NW</sub>/ITO electrodes.

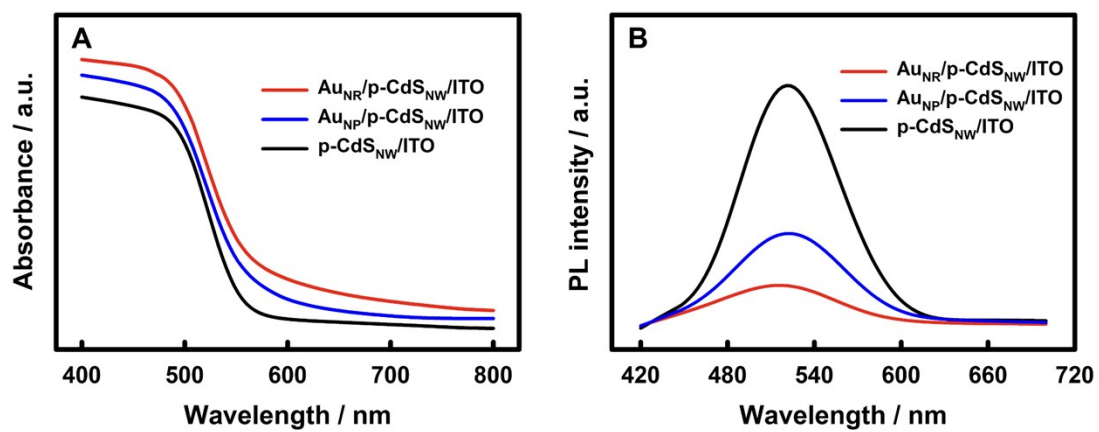


**Fig. S4.** UV-vis DRS (A) and PL spectra (B) for the p-CdS<sub>NW</sub>/ITO, Au<sub>NP</sub>/p-CdS<sub>NW</sub>/ITO and Au<sub>NR</sub>/p-CdS<sub>NW</sub>/ITO electrodes.

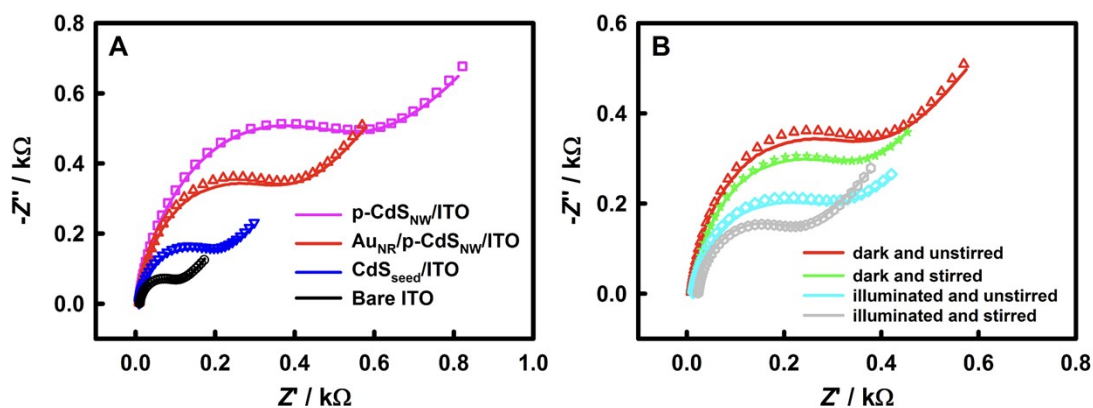


**Fig. S5.** (A) EIS results of the bare ITO, CdS<sub>seed</sub>/ITO, p-CdS<sub>NW</sub>/ITO and Au<sub>NR</sub>/p-CdS<sub>NW</sub>/ITO electrodes in 0.5 M aqueous Na<sub>2</sub>SO<sub>4</sub> containing 2.0 mM K<sub>4</sub>[Fe(CN)<sub>6</sub>] under dark and unstirred conditions, (B) EIS results of the Au<sub>NR</sub>/p-CdS<sub>NW</sub>/ITO electrode in 0.5 M aqueous Na<sub>2</sub>SO<sub>4</sub> containing 2.0 mM K<sub>4</sub>[Fe(CN)<sub>6</sub>] either without stirring or stirred at 1500 rpm (dark and unstirred; dark and stirred; illuminated and unstirred; or illuminated and stirred).



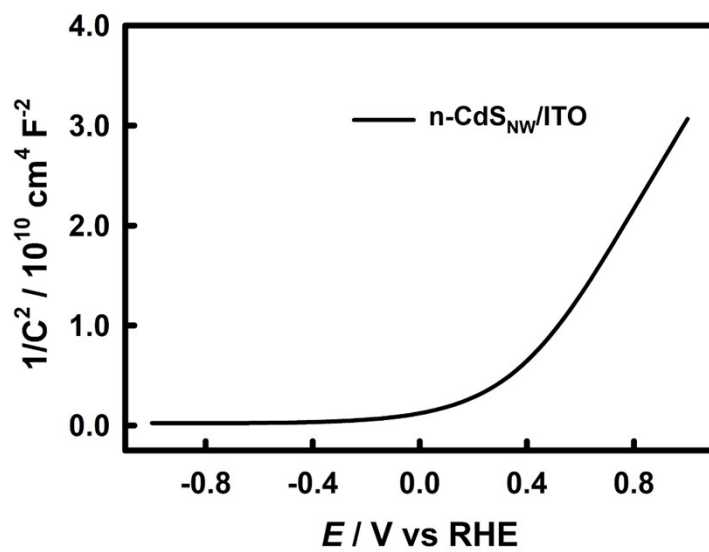


**Fig. S6.** Mott-Schottky curve for the n-CdS<sub>NW</sub>/ITO electrode.

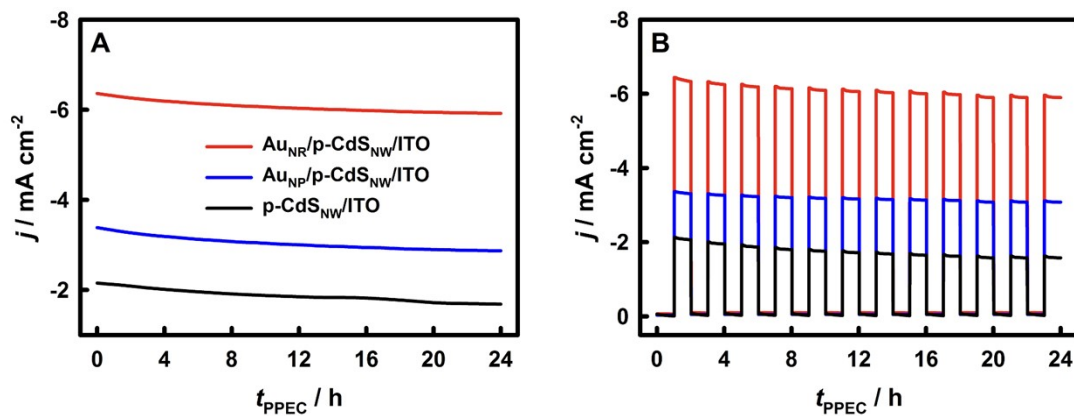


**Fig. S7.** (A)  $j$ - $t$  curves under continuous light illumination and (B)  $j$ - $t$  curves under chopped-light illumination (1 h switch time) of the Au<sub>NR</sub>/p-CdS<sub>NW</sub>/ITO, Au<sub>NP</sub>/p-CdS<sub>NW</sub>/ITO and p-CdS<sub>NW</sub>/ITO electrodes at 0.4 V vs RHE in O<sub>2</sub>-saturated 0.5 M aqueous Na<sub>2</sub>SO<sub>4</sub> stirred at 1500 rpm under 100 mW cm<sup>-2</sup> Xe lamp illumination.

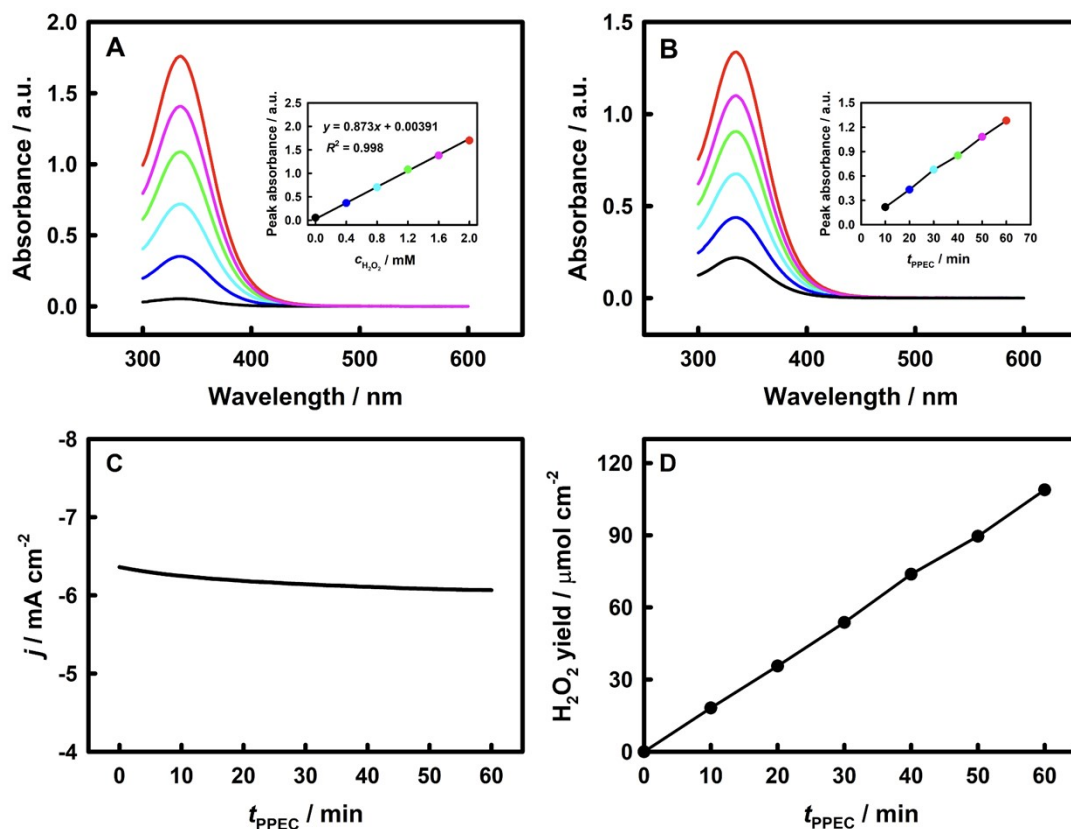


**Fig. S8.** UV-vis absorption spectra of  $\text{Fe}^{3+}$  generated by the  $\text{FeSO}_4\text{-H}_2\text{O}_2$  redox reaction for standard (A, a series of prepared standard  $\text{H}_2\text{O}_2$  solutions) or sample (B, the photocathode solution after different PPEC-ORR time)  $\text{H}_2\text{O}_2$  solutions. The insets show the linear relationship of the peak absorbance at 330 nm versus  $\text{H}_2\text{O}_2$  concentration ( $c_{\text{H}_2\text{O}_2}$ ) or PPEC-ORR time ( $t_{\text{PPEC}}$ ). Photocurrent density (C) and  $\text{H}_2\text{O}_2$  yield (D) on the  $\text{Au}_{\text{NR}}/\text{p-CdS}_{\text{NW}}/\text{ITO}$  electrode at 0.4 V vs RHE in  $\text{O}_2$ -saturated 0.5 M aqueous  $\text{Na}_2\text{SO}_4$  stirred at 1500 rpm under  $100 \text{ mW cm}^{-2}$  AM 1.5G simulated sunlight illumination. Here, the molar concentration of  $\text{H}_2\text{O}_2$  generated by PPEC and ORR is determined by UV-vis spectrophotometry of  $\text{Fe}^{3+}$  based on the  $\text{FeSO}_4\text{-H}_2\text{O}_2$  redox reaction. The molar concentration of  $\text{Fe}^{3+}$  ( $c_{\text{Fe}^{3+}}$ ) produced after the  $\text{FeSO}_4\text{-H}_2\text{O}_2$  redox reaction can be calculated according to the Lambert-Beer law.

The corresponding molar quantity of  $\text{H}_2\text{O}_2$  ( $n$ ) can be obtained by UV-vis spectrophotometry of  $\text{Fe}^{3+}$  based on the  $\text{FeSO}_4\text{-H}_2\text{O}_2$  redox reaction  $2\text{Fe}^{2+} + \text{H}_2\text{O}_2 + 2\text{H}^+ = 2\text{Fe}^{3+} + 2\text{H}_2\text{O}$ . The electric charge ( $Q'$ ) corresponding to the ORR generation of  $n$  mol  $\text{H}_2\text{O}_2$  can be obtained from the Faraday law of electrolysis,  $Q' = zFn$ , where  $z$  is the number of electrons transferred during ORR ( $z = 2$ ) and  $F$  is the Faraday constant ( $96485.3 \text{ C mol}^{-1}$ ). The Faraday efficiency ( $\eta$ ) is calculated according to  $\eta = Q'/Q \times 100\%$ .

At 60 min in Fig. S8B, we obtain  $n = 108.9 \mu\text{mol}$ ,  $Q' = 21.01 \text{ C}$ , and  $Q = 22.07 \text{ C}$ , so  $\eta = 95.2\%$ .

## Reference

1. L. Pan, S. C. Sun, Y. Chen, P. H. Wang, J. Y. Wang, X. W. Zhang, J. J. Zou and Z. L. Wang, *Adv. Energy Mater.*, 2020, **10**, 2000214.